Residual Strain in a Nb_3Sn Strand Mounted on a Barrel for Critical Current Measurements

Ludovic Thilly, Christian Scheuerlein, Uwe Stuhr, Bernardo Bordini, and Bernd Seeber

***Abstract*—The strain dependence of the critical properties of Nb_3Sn superconducting strands is a major complication for critical current (I_c) measurements. We report neutron diffraction measurements that have been carried out at room temperature and at 10 K in order to determine the strain state of a Nb_3Sn powder-in-tube (PIT) strand mounted on a critical current measurement barrel made out of a Ti-6Al-4V alloy.**

***Index Terms*—Diffraction, superconducting wires and filaments.**

I. Introduction

BECAUSE of the uncertainty of the 3-D strain state in Nb_3Sn superconducting strands that are mounted on measurement barrels, standardized I_c measurements can only provide relative values that allow a comparison between different strand designs and processing schemes. The stress in the Nb_3Sn strands on measurement barrels is influenced for instance by the mismatch of thermal expansion coefficients of the different strand constituents and the measurement barrel material. The bonding techniques used to fix the strand in order to inhibit strand movement can influence the I_c results as well.

Neutron diffraction measurements can been used for determining the residual strain in the different phases of Nb_3Sn strands [1], [2]. Here we report neutron diffraction measurements that have been carried out at room temperature (RT) and at 10 K in order to determine the strain state of the different phases in a Nb_3Sn powder-in-tube (PIT) strand mounted on a critical current measurement barrel made of Ti-6Al-4V alloy.

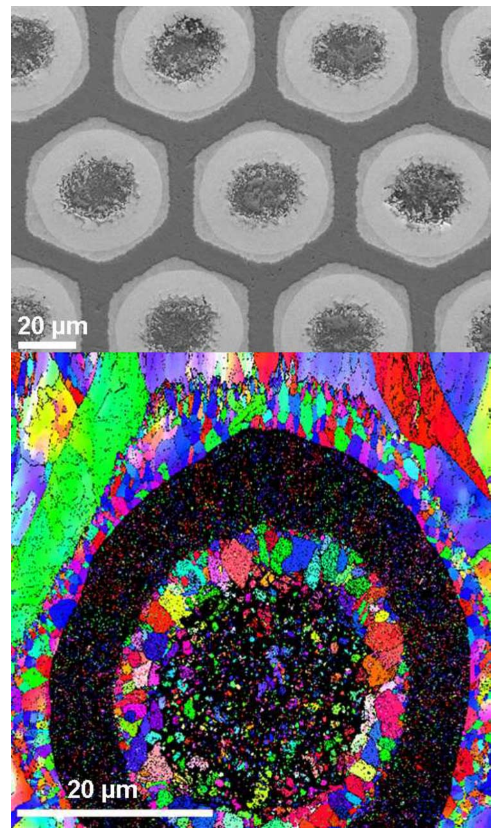

Fig. 1. Transverse cross section of the reacted PIT B215 strand. In the backscatter electron image (top) the different strand phases $(Nb-Ta)_3Sn$, Nb-Ta and Cu can be distinguished. The electron backscatter diffraction image (bottom) shows the grain orientation distribution in the different strand phases and allows to distinguish between the fine and coarse grain $(Nb-Ta)_3Sn$ areas. Courtesy G. Nolze, Federal Laboratory for Materials Research, Berlin.

II. Experimental

A. The Sample

The PIT strand B215 has been manufactured by Shape Metal Innovation (SMI), B. V., the Netherlands (now European Advanced Superconductors (EAS), Germany). The wire consists of 288 Nb-7.5wt.% Ta tubes that are filled with a powder containing NbSn2 and Sn particles. The Nb-7.5wt.% Ta tubes are embedded in a high purity Cu matrix. The non-reacted strand has a diameter of $\varnothing = 1.259 \pm 0.0004$ mm. The Cu to non-Cu volume ratio of the non-reacted strand determined by the Cu weight loss measurement is $R = 1.218$.

The strand has been studied after a 44 h-695°C heat treatment (HT). A transverse cross section of the fully reacted PIT strand is shown in Fig. 1. The Electron Backscatter Diffraction (EBSD) image in Fig. 1 shows the grain size and grain orientation distribution in the different strand phases.

The room temperature tensile properties of the PIT B215 strand have been determined by tensile tests. The engineering stress-strain curve of the reacted PIT B215 strand is shown in Fig. 2. The stress has been partly released every 0.02% in order to measure the apparent composite E-modulus as a function of

Manuscript received August 22, 2008. First published June 30, 2009; current version published July 15, 2009.

L. Thilly is with the Université de Poitiers, SP2MI, 86962 Futuroscope, France (e-mail: ludovic.thilly@univ-poitiers.fr).

C. Scheuerlein and B. Bordini are with the Accelerator Technology Department, CERN, CH-1211 Geneva 23, Switzerland (e-mail: Christian.Scheuerlein@cern.ch; bernardo.bordini@cern.ch).

U. Stuhr is with the ETHZ and Paul Scherrer Institut, CH-5232 Villigen, Switzerland (e-mail: uwe.stuhr@psi.ch).

B. Seeber is with the Institute of Applied Physics, University of Geneva, CH-1211 Geneva 4, Switzerland (e-mail: Bernd.Seeber@uni-ge.ch).

Color versions of one or more of the figures in this paper are available online at http://ieeexplore.ieee.org.

Digital Object Identifier 10.1109/TASC.2009.2019598

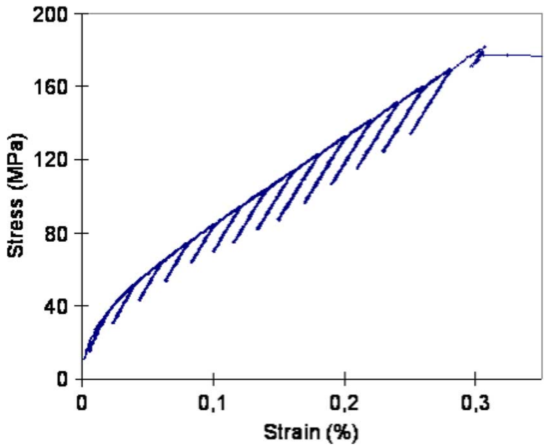

Fig. 2. Engineering stress-strain curve of the reacted PIT B215 composite strand measured at RT. The stress has been partly released every 0.02% in order to measure the apparent composite E-modulus as a function of axial composite strain. Courtesy B. Rehmer and M. Finn, Federal Laboratory for Materials Research, Berlin.

axial composite strain. With increasing composite strain the apparent E-modulus determined from the slope of the unloading curve decreases, possibly because of strain induced damage of the brittle Nb_3Sn phase. The apparent E-modulus measured at 0.2% strain is 116±0.3 GPa.

For I_c measurements the Nb_3Sn strand is wound onto a measurement barrel made of a Ti-6Al-4V alloy (see Fig. 3). This alloy has a similar thermal expansion coefficient as the Nb_3Sn phase in the reacted strand. At both ends of the barrel Cu rings are fixed to which the strand extremities are attached. During the reaction HT the strand ends are connected to the two Cu rings by means of two screws and after the HT and before the critical current measurement the wire ends are soldered to the Cu rings using a Sn-Ag alloy. The neutron diffraction measurements have been carried out with the strand ends soldered to the Cu rings.

Fig. 3. Sample holder for critical current measurements of Nb_3Sn superconducting strands. The PIT strand is wound onto a grooved Ti-6Al-4V cylinder with an outer diameter of 32 mm. After the reaction HT the wire is soldered onto Cu cylinders at both ends of the barrel.

B. Neutron Powder Diffraction

High resolution neutron powder diffraction measurements have been performed with the time-of-flight diffractometer with multiple pulse overlap (POLDI) [3], [4] at the Swiss spallation neutron source (SINQ) of the Paul Scherrer Institut (PSI) (Fig. 4).

In order to determine the transverse and axial lattice constants in the different strand phases, measurements were performed in two configurations with neutrons scattering at crystallographic planes either parallel or perpendicular to the strand axis (in the following referred to as transverse and axial directions, respectively). The instrument was calibrated using Si-powder from the National Institute of Standards and Technology (NIST standard Reference Material 640c).

For cooling, the VAMAS sample holder was mounted onto the cold head of a closed cycle cryo-cooler from CTI Cryogenics. The sample holder could be cooled down from room temperature (RT) to 10 K within 90 minutes.

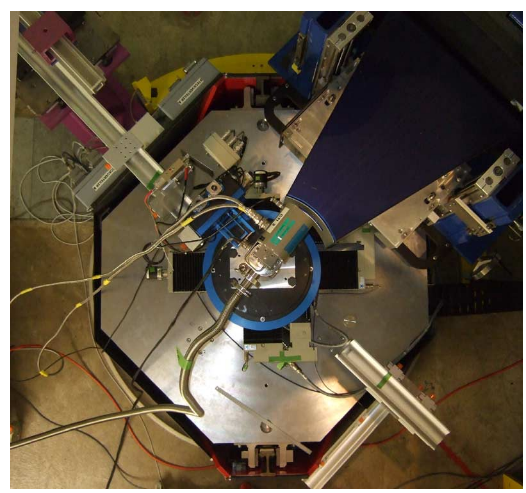

Fig. 4. Top view on the POLDI detector, the radial collimator and the sample area with the attached cryo-cooler.

III. Results

A. Axial and Transverse Lattice Parameters After the First Cool Down From the Reaction Temperature to RT

The lattice parameters for $(Nb-Ta)_3Sn$, Nb-Ta and Cu in axial and transverse wire direction measured at RT after cool down from the processing temperature are summarized in Table I. The lattice parameters are compared with the nearly stress free $(Nb-Ta)_3Sn$ and Nb-Ta lattice parameters obtained previously at POLDI using filaments that have been extracted from the Cu matrix of a similar PIT strand by chemical etching. The Nb-Ta and $(Nb-Ta)_3Sn$ lattice constants measured in the extracted tubes are 3.3009 Å and 5.2886 Å, respectively

TABLE I
LATTICE PARAMETERS MEASURED AT RT FOR THE DIFFERENT PHASES IN THE Nb_3Sn STRAND MOUNTED ON THE CRITICAL CURRENT MEASUREMENT BARREL. THE NB-TA AND $(Nb-Ta)_3Sn$ LATTICE PARAMETERS ARE COMPARED WITH THE CORRESPONDING NEARLY STRESS FREE LATTICE PARAMETERS (3.3009 Å AND 5.2886 Å, RESPECTIVELY)

	Lattice parameter in Å at RT
$(Nb-Ta)_3Sn$ (440) axial	5.2813±0.00081 -0.14%
$(Nb-Ta)_3Sn$ (321) transverse	5.2929±0.00081 +0.08%
Nb-Ta (110) axial	3.2968±0.00050 -0.12%
Nb-Ta (220) axial	3.2969±0.00047 -0.12%
Nb-Ta (211) transverse	3.3031±0.00054 +0.07%
Nb-Ta (110) transverse	3.3040±0.00048 +0.09%
Cu (111) axial	3.6165±0.00010
Cu (200) axial	3.6172±0.00029
Cu (111) transverse	3.6158±0.00013
Cu (200) transverse	3.6155±0.00023

TABLE II
LATTICE PARAMETERS OF THE DIFFERENT PHASES IN THE Nb_3Sn STRAND MOUNTED ON THE CRITICAL CURRENT MEASUREMENT BARREL MEASURED AFTER THE 1ST COOL DOWN OF THE SAMPLE HOLDER TO 10 K. THE LATTICE PARAMETERS ARE COMPARED WITH THE CORRESPONDING VALUES MEASURED AT RT, PRIOR TO THE 1ST COOL DOWN

	Lattice parameter in Å at 10 K
$(Nb-Ta)_3Sn$ (440) axial	5.2719±0.00092 -0.18%
$(Nb-Ta)_3Sn$ (321) transverse	5.2825±0.00108 -0.20%
Nb-Ta (110) axial	3.2907±0.00042 -0.19%
Nb-Ta (220) axial	3.2908±0.00034 -0.18%
Nb-Ta (211) transverse	3.2986±0.00083 -0.14%
Nb-Ta (110) transverse	3.2991±0.00045 -0.15%
Cu (111) axial	3.6053±0.00010 -0.31%
Cu (200) axial	3.6063±0.00028 -0.30%
Cu (111) transverse	5.2719±0.00092 -0.34%
Cu (200) transverse	5.2825±0.00108 -0.34%

[2]. It is assumed that these values correspond to the lattice parameters in a nearly stress free state at RT.

In axial direction the Nb_3Sn lattice parameter is about 0.14% smaller than the nearly stress free parameter while in transverse direction it is about 0.08% larger. Thus, in the PIT strand mounted on the VAMAS sample holder at RT $(Nb-Ta)_3Sn$ is under about 0.14% compressive axial pre-strain. Similar differences are found for the respective Nb lattice parameters (-0.12% and $+0.08\%$).

At RT (before the 1st cool down to 10 K) the Cu lattice parameter is in axial direction about 0.03% larger than in transverse direction, indicating that the Cu matrix is under axial tensile stress.

B. Influence of First Cool Down From RT to 10 K on the Axial Pre-Strain in the Different Strand Phases

The lattice parameters of the different strand phases measured at 10 K after the 1st cool down are presented in Table II. The lattice parameter variation between the values measured at 10 K and RT is presented as well.

The transverse lattice parameter variations during cool down from RT to 10 K measured with POLDI are in good agreement with the lattice parameter variations that are predicted from published thermal contraction factors (-0.18%, -0.15% and -0.3% for Nb_3Sn, Nb and Cu, respectively [5]).

During the 1st cool down from RT to 10 K the difference between the axial and transverse Nb_3Sn lattice parameters remains nearly constant, indicating that the residual compressive Nb_3Sn strain in axial direction is only slightly changed during the 1st cool down from RT to 10 K.

C. Influence of Thermal Cycling on the Axial Pre-Compression in the Different Strand Phases

In order to study a possible influence of thermal cycling on the Nb_3Sn lattice parameters at 10 K, lattice parameters have been re-measured after a second cool down from RT to 10 K and after subsequent heating of the sample holder to RT. The differences of the lattice parameters measured after the 1st and 2nd cool down to 10 K are relatively small and are approaching the resolution of the experiment. Nevertheless, the diffraction results indicate a significant reduction of the Nb_3Sn axial compressive pre-strain by thermal cycling between RT and 10 K.

D. Strand Length and Cross Section Changes During the Reaction HT of the Free Standing PIT Strand

After the strand reaction HT the PIT B215 strand length is reduced by about 0.15% with respect to the non-heat treated strand. After a 6 h-200°C annealing HT a similar contraction of 0.17% is measured (the estimated accuracy of the contraction measurement is $\pm 0.04\%$). Thus, it can be concluded that the strand contraction is caused by the Nb-Ta tube relaxation during the Cu annealing heat treatment, while the Nb_3Sn formation has only a minor influence. A similar contraction is observed for cold drawn Nb-Ti/Cu and Nb/Cu binary composite wires. The axial tensile stress of the Nb-Ta tubes develops during the cold working of the strand as a result of the plastic mismatch of Nb-Ta tubes and the Cu matrix [6]. During the reaction HT the strand diameter increases by 1.6% to $\varnothing = 1.280 \pm 0.0008$ mm, which corresponds with a cross section increase of 3.4%.

The non-Cu cross section increases by about 7% (mainly due to the presence of porosity in the reacted non-Cu part). In contrast, the Cu cross section increases only slightly by 0.15% because of the strand contraction. Thus, the true Cu to non-Cu volume ratio in the reacted strand is somewhat smaller than the ratio determined for the non-reacted strand ($R_{reacted} = 1.137$ vs. $R_{non-reacted} = 1.218$, respectively).

IV. Discussion and Conclusion

The $(\mathrm{Nb-Ta})_3\mathrm{Sn}$ phase in the PIT B215 strand mounted on the VAMAS sample holder is at RT under about 0.14% axial compressive pre-strain.

In contrast, the $(\mathrm{Nb-Ta})_3\mathrm{Sn}$ lattice parameters measured with POLDI in a straight free standing PIT strand show that in this case $(\mathrm{Nb-Ta})_3\mathrm{Sn}$ is not under axial pre-compression, but may be even under slight axial tension [2]. A slight axial tension of $\mathrm{Nb_3Sn}$ in the free standing PIT strand might be explained by the stronger $\mathrm{Nb_3Sn}$ thermal contraction with respect to the contraction of the unreacetd Nb barrier, assuming that the fully annealed Cu strand part is so soft that it cannot transmit stresses onto the filaments during the cool down from the processing temperature to RT.

The difference between the results obtained for the free standing PIT strand and the PIT strand reacted on the VAMAS barrel may be related to the fact that in the latter case the strand ends are fixed to the measurement barrel, which inhibits the strand contraction of about 0.15%, which takes place during the reaction HT of the free standing strand [7], [8].

Thermal cycling between RT and 10 K can affect the axial pre-strain in the A15 phase. Changes of the axial $\mathrm{Nb_3Sn}$ pre-strain have been reported to occur also under cyclic tensile loading [9] and bending [10] of bronze route strands at RT. A reduction of the axial pre-strain in the A15 phase should cause a measurable increase of I_c after the 2nd cool down, with respect to I_c measured after the 1st cool down.

Acknowledgment

The authors thank B. Rehmer and M. Finn from the Federal Laboratory for Materials Research (BAM), Berlin, for the tensile tests and G. Nolze from the BAM for the EBSD measurements. We are grateful to A. Godeke for stimulating discussions and suggestions.

The authors acknowledge the PSI for beam time at the POLDI experiment.

References

[1] R. Flükiger, W. Schauer, W. Specking, L. Oddi, L. Pintschovius, W. Mullner, and B. Lachal, *Adv. Cryo. Eng.*, vol. 28, pp. 361–370, 1982.

[2] C. Scheuerlein, U. Stuhr, and L. Thilly, "In-situ neutron diffraction under tensile loading of powder-in-tube $\mathrm{Cu/Nb_3Sn}$ composite wires: Effect of reaction heat treatment on texture, internal stress state and load transfer," *Appl. Phys. Lett.*, vol. 91, no. 4, p. 042503, 2007.

[3] U. Stuhr, *Nuclear Instruments and Methods in Physics Research A*, vol. 545, pp. 319–329, 2005.

[4] U. Stuhr, H. Spitzer, J. Egger, A. Hofer, P. Rasmussen, D. Graf, A. Bollhalder, M. Schild, G. Bauer, and W. Wagner, *Nuclear Instruments and Methods in Physics Research A*, vol. 545, pp. 330–338, 2005.

[5] N. Mitchell, "Finite element simulations of elasto-plastic processes in $\mathrm{Nb_3Sn}$ strands," *Cryogenics*, vol. 45, no. 7, pp. 501–515, 2005.

[6] L. Thilly, P. O. Renault, S. Van Petegem, S. Brandstetter, B. Schmitt, H. Van Swygenhoven, V. Vidal, and F. Lecouturier, "Evidence of internal bauschinger test in nanocomposite wires during in situ macroscopic tensile cycling under synchrotron beam," *Applied Physics Letters*, vol. 90, p. 241907, 2007.

[7] M. Pojer and L. Rossi, Development and Characterisation of ITD Multifilamentary $\mathrm{Nb_3Sn}$ Superconductors for 10–15 T Field Magnets INFN report, INFN/TC-99/25, 1999.

[8] D. R. Dietderich, J. R. Litty, and R. M. Scanlan, "Dimensional changes of $\mathrm{Nb_3Sn}$, $\mathrm{Nb_3Al}$, and $\mathrm{Bi_2Sr_2CaCu_2O_8}$ conductors during heat treatment and their implication for coil design," *Adv. Cryo. Eng.*, vol. 44b, pp. 1013–1020.

[9] S. Ochiai and K. Osamura, "Influence of cyclic loading at room temperature on critical current of $\mathrm{Nb_3Sn}$ superconducting composite wire," *Cryogenics*, vol. 32, pp. 584–590, 1992.

[10] S. Awaji, H. Oguro, G. Nishijama, P. Badica, K. Watanabe, S. Harjo, T. Kamiyama, and K. Katagiri, "Neutron diffraction study of prebending effects for bronze route $\mathrm{Nb_3Sn}$ wires without reinforcement," *IEEE Trans. Appl. Supercond.*, vol. 16, no. 2, pp. 1228–1231, 2006.